Essential function of *Drosophila* Sec6 in apical exocytosis of epithelial photoreceptor cells

Slobodan Beronja,[1] Patrick Laprise,[1] Ophelia Papoulas,[2,3] Milena Pellikka,[1] John Sisson,[2,3] and Ulrich Tepass[1]

[1]Department of Zoology, University of Toronto, Toronto, Ontario M5S 3G5, Canada
[2]The Section of Molecular Cell and Developmental Biology and [3]The Institute for Cellular and Molecular Biology, The University of Texas at Austin, Austin, TX 78712

Polarized exocytosis plays a major role in development and cell differentiation but the mechanisms that target exocytosis to specific membrane domains in animal cells are still poorly understood. We characterized *Drosophila* Sec6, a component of the exocyst complex that is believed to tether secretory vesicles to specific plasma membrane sites. *sec6* mutations cause cell lethality and disrupt plasma membrane growth. In developing photoreceptor cells (PRCs), Sec6 but not Sec5 or Sec8 shows accumulation at adherens junctions. In late PRCs, Sec6, Sec5, and Sec8 colocalize at the rhabdomere, the light sensing subdomain of the apical membrane. PRCs with reduced Sec6 function accumulate secretory vesicles and fail to transport proteins to the rhabdomere, but show normal localization of proteins to the apical stalk membrane and the basolateral membrane. Furthermore, we show that Rab11 forms a complex with Sec5 and that Sec5 interacts with Sec6 suggesting that the exocyst is a Rab11 effector that facilitates protein transport to the apical rhabdomere in *Drosophila* PRCs.

Introduction

Plasma membrane domains of polarized cells display distinct protein and lipid compositions. One critical mechanism that contributes to the formation and maintenance of membrane domains is targeted exocytosis of transport vesicles from the biosynthetic pathway or the recycling endosome (RE; for review see Mostov et al., 2003; Rodriguez-Boulan et al., 2004; Schuck and Simons, 2004). Genetic analysis in yeast has identified mutants in which bud growth is stalled and secretory vesicles accumulate below the bud site (Novick et al., 1980; for reviews see Finger and Novick 1998; Hsu et al., 2004). Eight of these genes encode components of the exocyst (or Sec6/8) complex (Sec3p, Sec5p, Sec6p, Sec8p, Sec10p, Sec15p, Exo70p, and Exo84p) that localizes to the bud site and apparently promotes the tethering of exocytotic vesicles to the plasma membrane before SNARE-mediated fusion.

Recent work has initiated the characterization of exocyst components in mammals and *Drosophila*. In contrast to yeast cells, where the exocyst contributes to all major secretory events, the metazoan exocyst appears to have more specialized functions. In neurons, for example, the exocyst has been implicated in neurite outgrowth and in the targeting of glutamate receptors to the synapse but a general role in neurotransmission has not been detected (Hazuka et al., 1999; Vega and Hsu, 2001; Sans et al., 2003; Murthy et al., 2003). Similarly, the exocyst is essential for transport of proteins to the basolateral membrane in mammalian epithelial cell culture systems, but not the apical membrane (Grindstaff et al., 1998). Cooperative action of E-cadherin and nectin, the two adhesion receptors found at the epithelial zonula adherens (ZA), recruits the exocyst to the apical junctional complex rapidly after cell contact formation (Yeaman et al., 2004). During branching morphogenesis of MDCK epithelial cysts in 3D culture, the exocyst can relocalize away from the apical junctional complex toward regions on the basolateral membrane that undergo rapid growth (Lipschutz et al., 2000). Regulation of exocyst function in both yeast and mammals involves a number of small GTPases including members of the Rab and Rho families (Lipschutz and Mostov, 2002; Inoue et al., 2003; Prigent et al., 2003). Nevertheless, the function and regulation of the metazoan exocyst in plasma membrane remodeling remains largely unresolved.

The yeast exocyst is not only involved in all major exocytotic events, but each of the eight exocyst components is essential for targeted exocytosis (Finger and Novick, 1998; Hsu et al., 2004). Whether such functional uniformity is also found in multicellular organisms remains unclear. Initial genetic analysis in *Drosophila* raises the possibility that significant functional diversification of exocyst components may have taken place. Although Sec5 is broadly required for exocytosis and cell

Correspondence to Ulrich Tepass: utepass@zoo.utoronto.ca

Abbreviations used in this paper: AEL, after egg laying; RE, recycling endosome; Arm, Armadillo; Crb, Crumbs; Chp, Chaoptin; Dαcat, Dα-catenin; DEcad, DE-cadherin; MF, morphogenetic furrow; PD, pupal development; Rh1, Rhodopsin 1; PRC, photoreceptor cell; ZA, zonula adherens.

The online version of this article contains supplemental material.

The Journal of Cell Biology, Vol. 169, No. 4, May 23, 2005 635–646
http://www.jcb.org/cgi/doi/10.1083/jcb.200410081

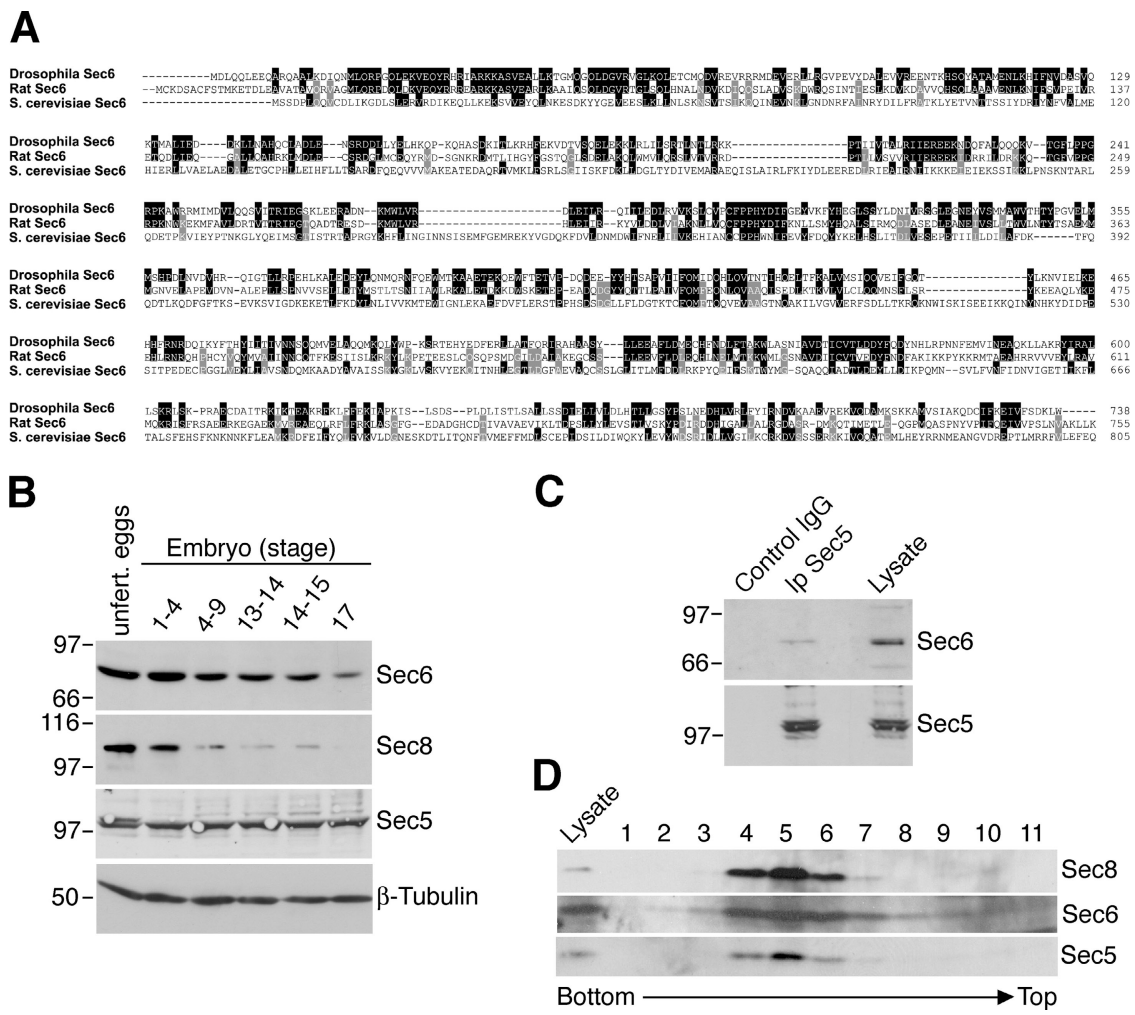

Figure 1. ***Drosophila* Sec6 is ubiquitously expressed and interacts with Sec5.** (A) Protein sequence alignment of *Drosophila*, rat, and yeast Sec6. (B) Developmental immunoblot detecting Sec6, Sec8, and Sec5 in unfertilized eggs and embryos. Sec6 (81 kD) is present in unfertilized eggs and at decreasing levels throughout embryogenesis. The amount of Sec5 remains constant. Sec8 (107 kD) is also maternally provided, but its expression strongly decreases and is undetectable by the end of embryogenesis. (C) Co-IP using Sec5 mAb 16A2 precipitates Sec6 as detected by immunoblotting. (D) Density gradient cosedimentation of membranes shows that Sec6, Sec5, and Sec8 largely cofractionate. Note that Sec6 is found in more fractions than either Sec5 or Sec8.

survival in flies (Murthy et al., 2003; Murthy and Schwarz, 2004), Sec10 appears to have an essential function only in a very limited number of secretory events (Andrews et al., 2002). We have conducted a genetic analysis of *Drosophila sec6* in order to study Sec6 function and the role of polarized exocytosis. We also show interactions between the small GTPase Rab11 and the exocyst suggesting that the exocyst acts as a Rab11 effector.

Results

Drosophila Sec6 and Sec5 form a complex

The *Drosophila* genome project has identified homologues to all eight exocyst complex components known in yeast and mammals (Littleton, 2000; Murthy et al., 2003). We selected *sec6* as a target for our genetic analysis of exocyst function because a nearby P element insertion was available, that facilitated the generation of *sec6* mutations. *Drosophila* Sec6 shows 38% identity to rat Sec6, and 18% identity to yeast Sec6 (Fig. 1 A). Sec6 protein is present in unfertilized eggs, embryos (Fig. 1 B), larvae (Fig. 2 B) and adults (not depicted). Unfertilized eggs also contained Sec5 and Sec8. Although the concentration of Sec5 remains constant, Sec6 levels decrease, and the amount of Sec8 detected declines dramatically during the course of embryonic development (Fig. 1 B). Sec8 was undetectable in late embryos, larvae, and only minor amounts were seen in adult flies. These findings suggest that Sec6 and Sec5 are found throughout development, whereas Sec8 shows dramatic stage-specific differences in protein levels. Co-immunoprecipitation experiments using a Sec5 antibody (Murthy et al., 2003) precipitated Sec6 from embryonic lysates (stages 1–17; Fig. 1 C). In contrast, we were unable to detect Sec8 in our precipitates.

We also assessed the relative distribution of Sec6, Sec5, and Sec8 by membrane fractionation of 1–3-h-old embryos (stages 1–5), when the concentration of Sec8 is at its maximum (Fig. 1 D). A significant proportion of Sec6 did cosediment with Sec5 and Sec8, suggesting that they associate with a common, and relatively uniform, membrane population. The Sec6/

Sec5/Sec8 peak fractions were also enriched for the Golgi-associated proteins Lava lamp (Sisson et al., 2000), p120 (Stanley et al., 1997), and α-COP (Pavel et al., 1998; unpublished data), which is consistent with the possibility that the exocyst complex is largely associated with Golgi-derived membrane vesicles in pregastrulation embryos. Sec6 displays a broader sedimentation profile than Sec8 or Sec5, raising the possibility that Sec6 associates with additional membrane fractions independently of other exocyst components.

sec6 is an essential gene

We used imprecise excision of the viable P element insertion EP2021 (Rorth et al., 1998), which is located between *sec6* (*CG5341*) and *Eip55E*, to generate *sec6* mutations (Fig. 2 A). We isolated 72 deletion mutations in the region that were classified by complementation analysis and molecular characterization of the extent of the deletions. 14 mutations affect only *sec6*, 47 mutations affected only *Eip55E* and 11 mutations affected both genes. The largest deletion is $sec6^{175}$, which removes *Eip55E* entirely, and extends 1,720-bp upstream of the EP2021 insertion site, deleting 455 COOH-terminal aa of Sec6 (Fig. 2 A). $sec6^{20}$ is the largest deletion that only affects *sec6*, removing 242 COOH-terminal aa of Sec6. $sec6^{125}$, the smallest deletion of *sec6*, results in a loss of 62 COOH-terminal aa and introduction of six new aa.

Animals mutant for $sec6^{175}$ and $sec6^{20}$ complete embryogenesis but fail to grow as larvae and die at ~72 h after egg laying (AEL) when wild-type or heterozygous animals have reached the late second or early third larval instar. $sec6^{175}$ and $sec6^{20}$ behave as genetic null mutations for *sec6* as the homozygous and hemizygous phenotypes caused by these mutations are identical. $sec6^{125}$, our weakest allele appears to be a strong hypomorph; mutant animals also fail to grow as larvae but die only at ~96 h AEL. *sec6* mutant cell clones degenerate but can be rescued by a *UAS-sec6* transgene. These findings indicate that *sec6* is an essential gene and that we have isolated null mutations of *sec6*.

As expected, we found that maternally provided Sec6 protein declines in homozygous *sec6* mutant larvae (Fig. 2 B). Sec6 remains detectable in these animals even at 72 h AEL, when $sec6^{175}$ and $sec6^{20}$ mutants die, indicating that failure to grow and death occur before Sec6 is completely depleted. Our Sec6 antibodies are directed against a portion of Sec6 that is not deleted in the $sec6^{20}$ and $sec6^{125}$ alleles. However, we failed to detect truncated Sec6 protein in both mutants suggesting that these proteins are unstable. As mentioned, we did not detect Sec8 in extracts from whole larvae. In contrast, Sec5 is readily detectable and its levels remain normal in *sec6* mutants (Fig. 2 B), suggesting that the stability of Sec5 protein is not dependent on normal expression levels of Sec6.

Sec6 is required for plasma membrane growth in the female germline

Maternal expression of *sec6* supports normal embryogenesis. To investigate the requirement of *sec6* during embryonic development we removed the maternal component by generating germline clones for *sec6* mutations. However, germline clones for the three described *sec6* alleles did not produce eggs, indicating that *sec6* has an essential function in the development of the female germline. Sec6, Sec8, and Sec5 showed a diffuse, punctate distribution in the cytoplasm of germline cells of the germarium and follicles (Fig. 3 A and not depicted). Sec8 is found at very low levels in early follicles but is up-regulated between stages 7 and 10 when it is strongly enriched in the oocyte membrane that is in contact with follicle cells (Fig. 3 C′). The accumulation of Sec8 in the oocyte membrane coincides with a similar accumulation of Sec5 (Fig. 3 C; Murthy and Schwarz, 2004) but is not seen for Sec6 (Fig. 3 B). Furthermore, in contrast to Sec5, Sec8 is not found at the interface of oocyte and nurse cells. These data suggest that Sec6, Sec8, and Sec5 show overlapping but also distinct distribution patterns during oogenesis.

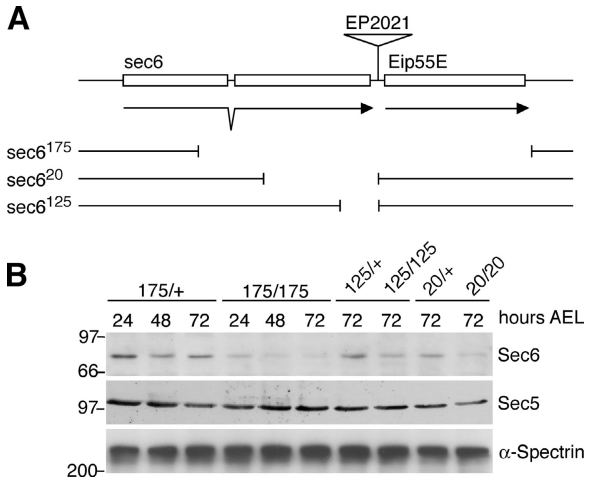

Figure 2. **Generation of *sec6* mutations.** (A) Extent of deletions $sec6^{175}$, $sec6^{20}$, and $sec6^{125}$ induced by imprecise excision of the EP2021 P element that maps between *sec6* and *Eip55E*. (B) Zygotic mutants for all three *sec6* alleles show a decrease of Sec6 whereas levels of Sec5 are not affected. AEL, after egg laying.

Early follicles containing a *sec6* mutant germline showed no apparent defects. However, as mutant follicles develop and germline cells increase in volume, membrane and membrane-associated markers such as F-actin, Patj (Tanentzapf et al., 2000), DE-cadherin (DEcad), and Con A failed to detect plasma membrane between germline cells by stage 6 or 7 (Fig. 3, D–G). Ring canals and associated molecules had collapsed to a single clump within the germline cyst, and nuclei showed an irregular arrangement. All three *sec6* alleles caused a similar phenotype and we did not observe any follicles with a *sec6* mutant germline past stage 7, suggesting that mutant follicles degenerate. The normal early development of *sec6* mutant germline clones could either indicate that *sec6* is not required during these stages or may be the result of perdurance of the *sec6* gene product. These findings suggest that Sec6, similar to Sec5 (Murthy and Schwarz, 2004), has a critical function in plasma membrane growth in the female germline consistent with an essential function in exocytosis.

Sec6 functions in apical protein transport in photoreceptor cells

To determine the role of Sec6 in a cell type that shows highly targeted secretion, we investigated the distribution and function of Sec6 in photoreceptor cells (PRCs). The retina develops

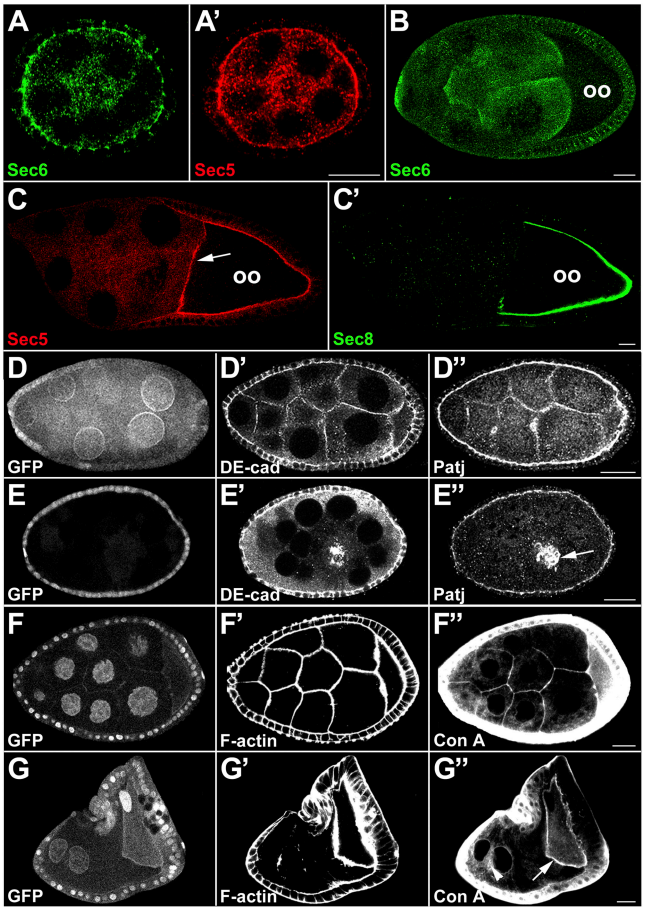

Figure 3. **Sec6 is required for plasma membrane integrity of the female germline.** (A) Sec6 and Sec5 show a punctate cytoplasmic distribution in the germline of early follicles. (B) Stage 9 follicle showing uniform, punctate distribution of Sec6 in nurse cells and the follicular epithelium and lower levels in the oocyte (oo). (C) Stage 9 follicle showing Sec8 and Sec5 accumulation at the oocyte membrane. Note that Sec8 levels in nurse cells and follicle cells are very low compared with Sec5 or Sec6 (B), and that Sec8 is not detected at the anterior oocyte membrane in contrast to Sec5 (arrow). (D and F) Wild-type follicle. (E and G) Follicles with a *sec6*^{20} mutant germline clone (E) or partially mutant germline clone (G) as identified by the absence of GFP. DEcad, Patj, F-actin, and Con A do not accumulate between *Sec6* mutant germline cells suggesting that plasma membranes are absent. Note that in the partial germline clone in G, plasma membrane is lost except around the oocyte (arrow) and a remnant of membrane between the two GFP-positive nurse cell nuclei (arrowhead). A central clump of material highlighted by DEcad (E′) and Patj (E′′) presumably represents collapsed ring canals (arrow). Bars, 20 μm.

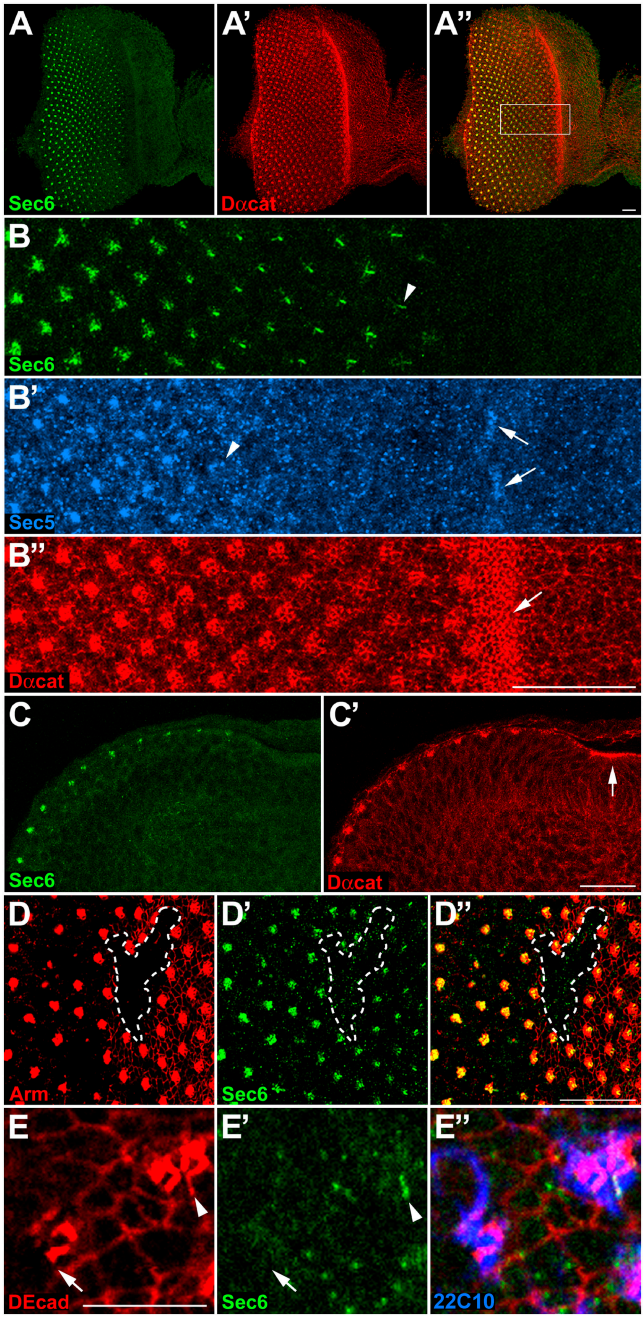

Figure 4. **Distribution of Sec6 in third larval instar eye discs requires Arm.** (A) Sec6 and Dαcat colocalize in the third larval instar eye disc. (B) Top view and (C) side view of a portion of a third larval instar eye imaginal disc (A′′, box) showing ~20 rows of PRC clusters posterior to the morphogenetic furrow (MF; B′′ and C′, arrows). The MF and PRCs show strong apical enrichment of Dαcat at the ZA. Sec6 colocalizes with Dαcat at the ZA two to four rows behind the MF (B, arrowhead). Some apical accumulation of Sec5 is already apparent in the MF (B′, arrows). However, within the PRC clusters, apical Sec5 accumulation is trailing that of Sec6 by several rows (B′, arrowhead). Apical Sec5 appears more diffuse than Sec6. (D) Clone of *arm*^{XP33} mutant eye disc cells marked by the loss of Arm (outline) does not show ZA enrichment of Sec6 (D′). (E) Clone of *arm*^{XP33} mutant eye disc cells marked by the loss of DEcad. PRCs are labeled with a neuronal marker 22C10 (E′′). DEcad (E) and Sec6 (E′) accumulation between wild-type PRCs (E and E′, arrowheads) is not seen at the interface between a wild-type and an *arm*^{XP33} mutant cell (E and E′, arrow). All images represent a projection of a 20-μm-deep series of Z-sections. Bars: (A–D) 20 μm; (E) 10 μm.

from a simple monolayered epithelium, the eye disc, that gives rise to PRCs and several types of accessory cells, such as the pigment cells. During the second half of pupal development (PD), PRCs form the rhabdomere, the light sensing organelle that is composed of densely packed microvilli. The rhabdomere is located in the center of the apical membrane surrounded by the stalk membrane that links the rhabdomere to the ZA and the basolateral membrane (Fig. 5 I). Massive targeted exocytosis is needed to build the rhabdomere and maintain the supply of the photopigment rhodopsin.

We examined Sec6, Sec5, and Sec8 expression at three stages of retinal development: at the third larval instar when PRCs are specified, at 55% PD when formation of the rhab-

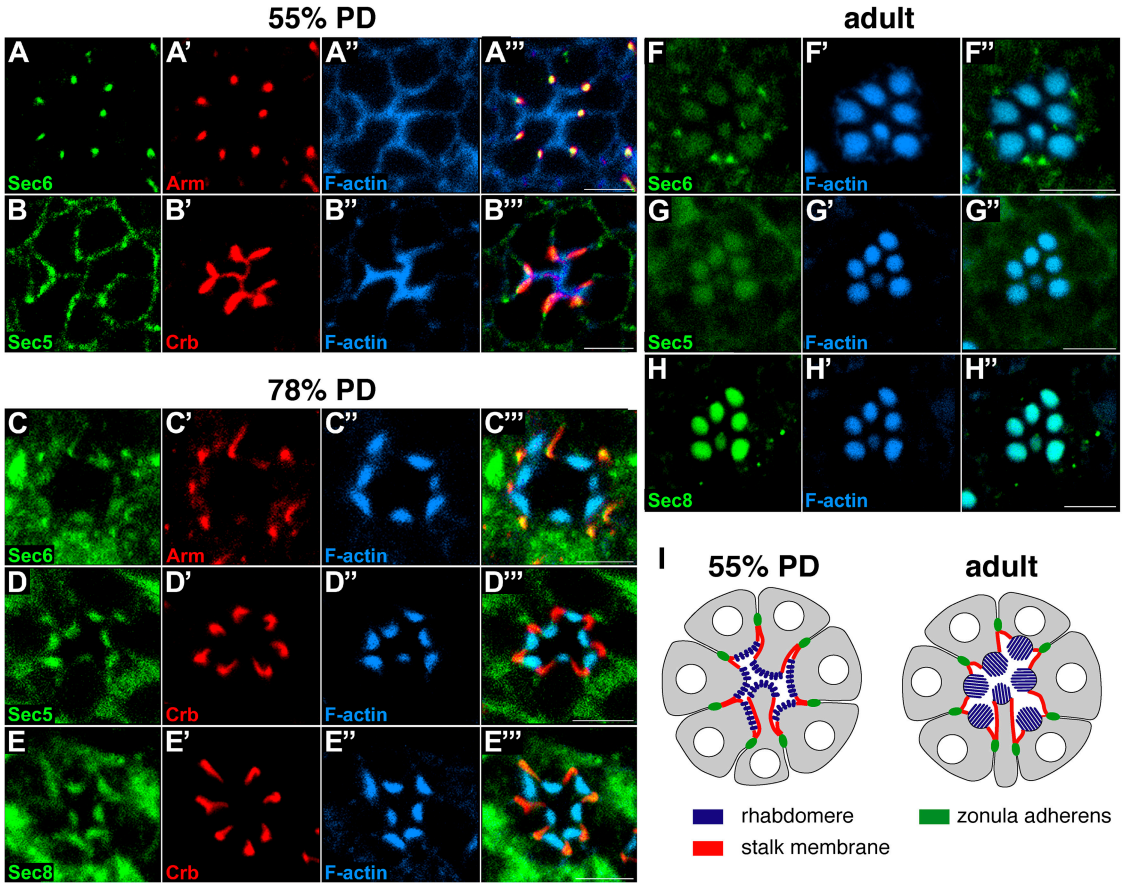

Figure 5. **Sec6, Sec5, and Sec8 distribution in pupal and adult PRCs.** All panels show optical cross sections through individual wild-type ommatidia at 55% PD (A and B), 78% PD (C–E), and adult (F–H). (A) Sec6 localizes to the ZA (marked by Arm) of PRCs at 55% PD. (B) Sec5 associates with the basolateral and apical membrane at 55% PD, and appears somewhat enriched at the apical membrane were it colocalizes with Crb at the stalk membrane. (C–H) Sec6, Sec5, and Sec8 localize to the rhabdomere, marked by strong labeling of F-actin with phalloidin. Sec6 also remains associated with the ZA, marked by Arm in C. None of the exocyst proteins show significant accumulation at the stalk membrane, marked by Crb in D and E. All three exocyst proteins are also found throughout the PRC cytoplasm. (I) Diagram of cross sections of an ommatidium at 55% PD and adult. The rhabdomere and the stalk membrane comprise the apical membrane of PRCs, whereas the ZA and the rest of the membrane comprise the basolateral membrane. Bars, 5 μm.

domere is initiated, and at 78% PD or later when rhabdomeres have formed and rhodopsin is being delivered to the rhabdomere (Kumar and Ready, 1995). Sec6 and Sec5 show a diffuse cytoplasmic distribution in most imaginal disc cells. In addition, Sec6 is strongly enriched at the ZA of larval PRCs (Fig. 4, A–C) and of pupal PRCs at 55% PD (Fig. 5 A). The apical accumulation of Sec6 is not seen in *armadillo* (*arm*) mutant clones consistent with the notion that adherens junctions recruit Sec6 (Fig. 4 D). However, the loss of Sec6 from *arm* mutant PRCs may be secondary as PRC differentiation appears abnormal in *arm* mutant clones. Wild-type PRCs next to *arm* mutant cells also fail to accumulate Sec6 at the adherens junction (Fig. 4 E) indicating that at least normal cell contact between PRCs is important for Sec6 recruitment. Sec5 is present along the apical and basolateral plasma membrane at these stages, but shows apical enrichment that colocalizes with Crumbs (Crb) in the stalk membrane (Figs. 4 B′ and Fig. 5 B). We did not detect Sec8 in larval eye discs or PRCs at 55% PD. In contrast, at 78% PD and in adults, all three exocyst proteins are now found in the rhabdomere and the cytoplasm of PRCs (Fig. 5, C–H). In addition, Sec6 continues to show robust ZA localization. None of the Sec proteins are detected at the stalk membrane. These findings show overlapping and distinct distributions of Sec6, Sec5, and Sec8, which is consistent with the possibility that the exocyst undergoes a dynamic reorganization during PRC morphogenesis, ultimately adopting a function in targeting secretory vesicles to the rhabdomere.

To analyze *sec6* function in PRC morphogenesis we induced *sec6* mutant cell clones in the developing retina. When *sec6* mutant clones are induced and wild-type sister clones (twin spots) are ablated, eye development is abolished (Fig. 6 B). The residual eye tissue seen in such flies is likely derived from a small number of disc cells that did not undergo mitotic recombination. Similar eye ablation defects are seen with all three *sec6* alleles. We did not recover *sec6* mutant cell clones in third larval eye discs or other imaginal discs (unpublished data), indicating that *sec6* is essential for cell proliferation or survival of eye disc cells. This situation did not allow us to examine *sec6* function in PRC morphogenesis.

To overcome this limitation we supplied Sec6 exogenously during larval stages and depleted Sec6 after growth and patterning of the eye disc had occurred in discs that con-

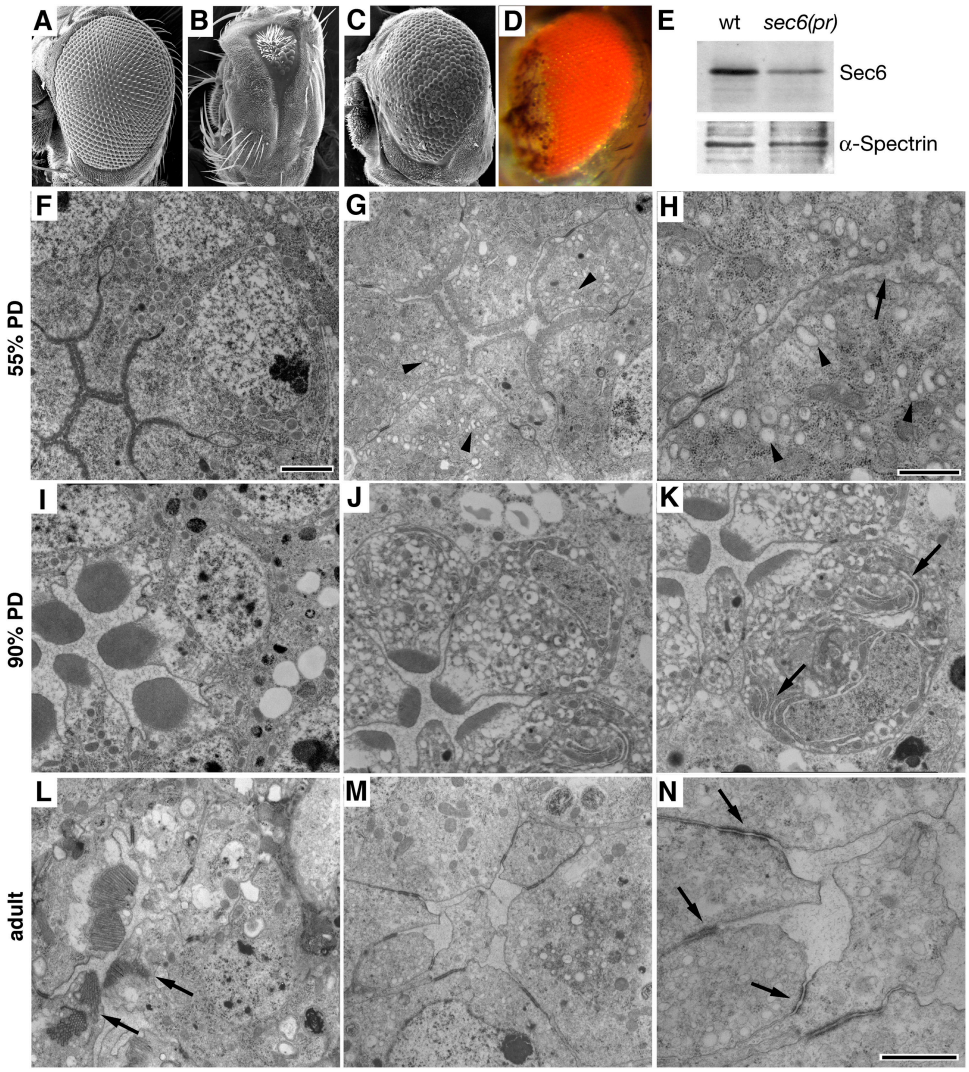

Figure 6. **Accumulation of secretory vesicles in *sec6(pr)* mutant PRCs.** (A–C) Scanning EM of a wild-type (A), *sec6*^{20} (B), and *sec6(pr)* mutant eyes (C). (D) Adult *sec6(pr)* mutant eye showing loss of pigment in the anterior. (E) Immunoblot showing that *sec6(pr)* mutant adult retinas have strongly decreased levels of Sec6 compared with wild type. (F–N) Transmission EM of wild-type (F and I) and *sec6(pr)* mutant PRCs (G, H, J–N) at 55% PD (F–H), 90% PD (I–K), and adult (L–N). *sec6(pr)* mutant PRCs show prominent groups of small vesicles (arrowheads) in the apical cytoplasm at 55% PD and gaps in the array of microvilli are seen (G and H; arrow). In wild type, such vesicles are rare and microvilli form a continuous rim (F). *sec6(pr)* mutant PRCs at 90% PD are filled with vesicles 100–300 μm in diameter and PRCs appear swollen (J and K) in contrast to wild type (I). Rhabdomeres in *sec6(pr)* mutant PRCs are small and flattened and some cells display an enlarged ER (K, arrows). Adult *sec6(pr)* mutant PRCs show strong reduction in size (L, arrows) or complete loss of rhabdomeres (M), but display normal ZAs (N, arrows). Bars: (F, G, and I–M) 1 μm; (H and N) 0.5 μm.

tained *sec6* mutant clones. We took advantage of an FLP recombinase driven by the Gal4/UAS system, where Gal4 expression is under the control of the *eyeless* (*ey*) promoter (Quiring et al., 1994; Stowers and Schwarz, 1999). Adding a *UAS-sec6* transgene supplies exogenous Sec6 activity while *sec6* mutant cell clones are being induced. Overexpression of Sec6 (*ey-Gal4 UAS-sec6*) in a wild-type background, did not result in detectable morphological defects suggesting that increasing Sec6 levels does not adversely affect eye development. This result is corroborated by the high-level overexpression of Sec6 in a variety of tissues and developmental stages or ubiquitous overexpression that also did not affect viability or morphology. *ey-Gal4* activity is high throughout the larval and early pupal stages, but by 30–40% PD its activity dramatically declines throughout the retina as revealed by a *UAS-lacZ* reporter; the posterior half of the retina maintains low levels of expression at this stage that further declines during the remainder of PD (Fig. S1, available at http://www.jcb.org/cgi/content/full/jcb.200410081/DC1). Thus, exogenous expression of Sec6 is expected to decline before mid-pupal stages, and we therefore anticipated that the effect of Sec6 depletion should manifest itself by mid-pupal stages and worsen as Sec6 levels progressively decline. We will refer to mutant clones generated using this strategy as *sec6(pr)* (for partial rescue).

sec6(pr) mutant eyes, in which wild-type twin spots were ablated, developed to near normal size in contrast to *sec6* mutant eyes (Fig. 6, B and C). Western blot analysis indicates that *sec6(pr)* mutant retinas have strongly decreased levels of Sec6 compared with wild type (Fig. 6 E). *sec6(pr)* mutant eyes are

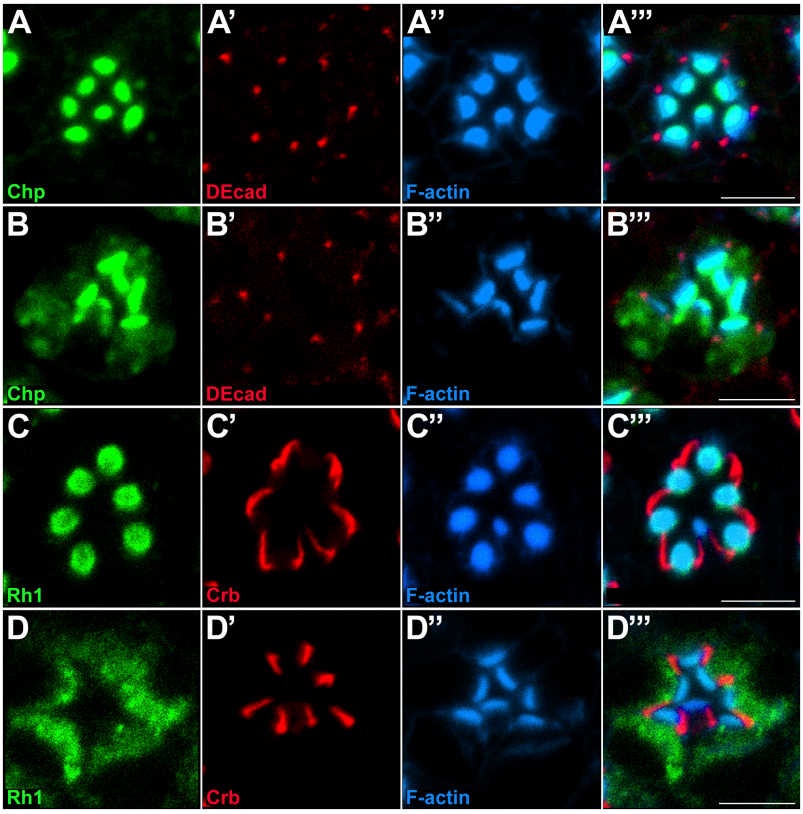

Figure 7. **Sec6 is required for protein transport to the rhabdomere.** Optical cross sections of individual wild-type (A and C) and *sec6(pr)* ommatidia (B and D) at 78% PD (A and B) or from 1-d-old adult eye (C and D). Chp (B) and Rh1 (D) accumulate in the cytoplasm of *sec6(pr)* mutant PRCs in contrast to wild type, whereas DEcad and Crb show normal subcellular distributions. Rhabdomeres are identified by labeling F-actin with phalloidin. Bars, 5 μm.

slightly rough and interommatidial bristles are virtually absent. Defects in the differentiation of the cornea and the pigment cells are apparent that are more severe in the anterior half of the eye, which is consistent with the profile of *ey-Gal4* activity (Fig. 6, C and D; Fig. S1). The defects in *sec6(pr)* mutant eyes are consistent with normal growth and patterning of the eye disc but abnormal terminal differentiation during later stages of PD.

sec6(pr) mutant PRCs were examined with transmission EM at 55% and 90% PD and in 1-d-old adult flies. Rhabdomere formation has just been initiated at 55% PD; apical surfaces of PRCs are decorated with short microvilli and the interrhabdomeral space is starting to emerge (Fig. 5 I and Fig. 6 F; Longley and Ready, 1995). Gross morphological defects are not apparent in *sec6(pr)* mutant PRCs at this stage but we note some defects in the organization of microvilli (Fig. 6 H) and a conspicuous increase in cytoplasmic vesicles (Fig. 6, G and H): 15.5 vesicles/cell/cross section profile ($n = 35$) compared with 1.7 vesicles in wild type ($n = 42$; Fig. 6 F). At 90% PD, rhabdomeres are fully formed in wild type displaying round profiles with an ~1-μm diam (Fig. 6 I). *sec6(pr)* mutant PRCs show smaller and flattened rhabdomeres (Fig. 6, J and K). In addition, the cytoplasm of *sec6(pr)* mutant PRCs is filled with vesicles of 100–300 nm in diameter that are only rarely seen in wild type (Fig. 6 I). This defect is highly reminiscent of the accumulation of cytoplasmic vesicles in yeast cells with compromised exocyst function (Novick et al., 1980). Also the proximal–distal length of adult rhabdomeres in *sec6(pr)* (41.0 μm; $n = 55$) was significantly reduced compared with wild type (81.6 μm; $n = 55$). The *sec6(pr)* retina as a whole reaches only approximately half the depth of a wild-type retina (not depicted). In some *sec6(pr)* PRCs, we also noted an enlarged ER (Fig. 6 K). Finally, PRCs and other cells of the retina show widespread signs of degeneration in 1-d-old flies. PRCs have either strongly reduced rhabdomeres (Fig. 6 L) or rhabdomeres are missing (Fig. 6 M). Interestingly, well-formed ZAs are still seen even in those PRCs that lack rhabdomeres (Fig. 6 N). Together, these findings suggest that Sec6 compromised PRCs show a massive failure in exocytosis. As the rhabdomeres in *sec6(pr)* mutant PRCs are much smaller than in wild type, but the stalk membrane and ZAs appear normal it seems likely that at least most of the cytoplasmic vesicles that accumulate in *sec6(pr)* mutant PRCs represent a rhabdomere-specific population of transport vesicles.

To address the question whether Sec6 is specifically involved in the targeting of rhabdomere proteins we examined the distribution of four transmembrane proteins in *sec6(pr)* mutant PRCs. Chaoptin (Chp) localizes specifically to the rhabdomere as it forms, but is expressed in PRCs already in the larval eye disc (Van Vactor et al., 1988). Rhodopsin 1 (Rh1) is the major photopigment in flies found in the PRCs R1 to R6 and is transported to the rhabdomere starting at ~78% PD (Kumar and Ready, 1995). Crb is a stalk membrane-specific marker and DEcad localizes to the ZA (Pellikka et al., 2002; Sang and Ready, 2002). Crb and DEcad show normal localization and no cytoplasmic accumulation in *sec6(pr)* mutant PRCs (Fig. 7, B′ and D′). In contrast, Chp and Rh1 accumulate in the cytoplasm of *sec6(pr)* mutant PRCs. Although Chp is still found in the rhabdomere, Rh1 accumulation in the rhabdomere is abolished completely (Fig. 7, B and D). This discrepancy is presumably

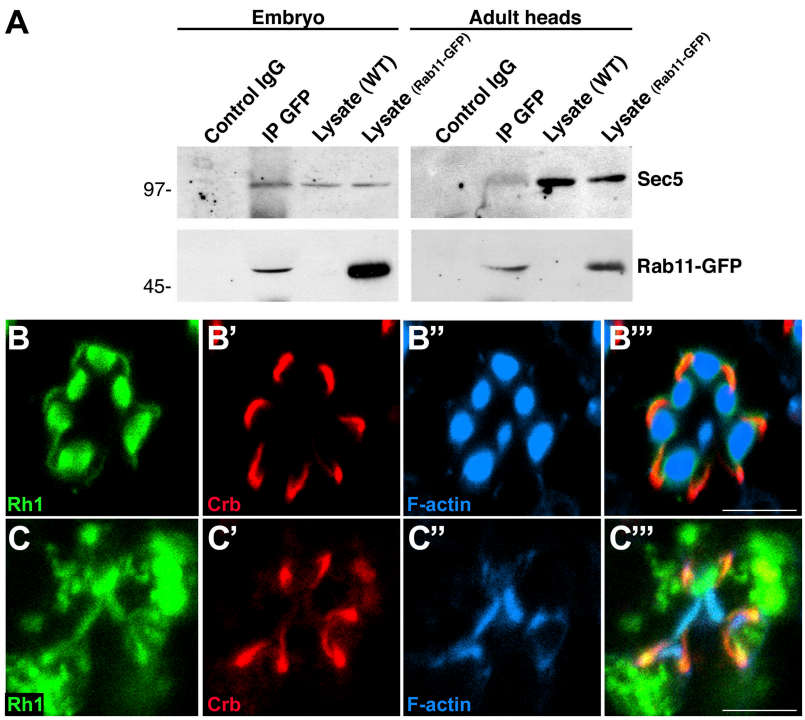

Figure 8. **The exocyst is a Rab11 effector and mediates direct Rh1 transport to the rhabdomere.** (A) Co-IP with anti-GFP mAb precipitates Sec5 from lysates of *da-Gal4 UAS-Rab11-GFP* embryos ubiquitously expressing Rab11::GFP and *Rh1-Gal4 UAS-Rab11-GFP* eyes expressing Rab11::GFP in PRCs R1-R6. (B) PRCs of shi^{ts2} adults grown at 29°C for 3 d show normal accumulation of Rh1 in the rhabdomeres. (C) PRCs of shi^{ts2} *sec6(pr)* flies grown at 29°C for 3 d show cytoplasmic accumulation of Rh1. Bars, 5 μm.

the consequence of the different temporal expression profiles of Chp and Rh1. Chp is expressed in larval and early pupal stages when Sec6 is still active in *sec6(pr)* mutant PRCs whereas by the time Rh1 becomes expressed at 78% PD, Sec6 activity has declined to an extent that blocks exocytosis. Together, these findings suggest that Sec6 acts specifically in targeting secretory vesicles to the rhabdomere in differentiating and mature PRCs.

Sec5 interacts with Rab11 in Golgi to rhabdomere traffic of Rh1

Two recent findings suggest that the small GTPase Rab11 may interact with exocyst proteins in *Drosophila* PRCs. First, depletion of Rab11 function in PRCs causes a mutant phenotype similar to that seen in *sec6(pr)* flies that is characterized by a massive accumulation of Rh1 containing secretory vesicles and small rhabdomeres (Satoh et al., 2005). Second, physical interactions between the exocyst protein Sec15 and Rab11 were found in mammalian culture cells (Zhang et al., 2004). To test for interactions between Rab11 and exocyst proteins in *Drosophila* PRCs we expressed GFP-tagged Rab11 in adult eyes and immunoprecipitated it with anti-GFP antibodies. These precipitates contained Sec5 (Fig. 8 A) but Sec6 was not detected. Similar results were obtained with embryonic extracts (Fig. 8 A). Together, the accumulation of rhabdomere-specific secretory vesicles seen in *Rab11* and *sec6(pr)* mutant PRCs and the physical interactions between Rab11 and Sec5 suggest that the exocyst is a Rab11 effector complex in PRCs and possibly other *Drosophila* tissues.

Rab11 localizes to the RE in many different cell types (Hoekstra et al., 2004). This raises the possibility that rhabdomere proteins are taking not a direct route from the Golgi to the apical membrane, but are delivered first to the basolateral membrane and then transcytosed to the apical membrane. This scenario seems unlikely as the expression of dominant-negative Rab5, which interferes with an early step in endocytotic trafficking, does not prevent Rh1 delivery to the rhabdomere (Bucci et al., 1992; Shimizu et al., 2003; Satoh et al., 2005). To further corroborate a direct Golgi to rhabdomere route for Rh1 we compromised endocytosis by disrupting the function of Dynamin. Flies that carried a temperature sensitive allele of *shibire* (shi^{ts2}), which encodes *Drosophila* Dynamin (Grigliatti et al., 1973; van der Bliek and Meyerowitz, 1991), and were maintained at the restrictive temperature (29°C) for 2 or 3 d during late PD showed normal localization of Rh1 to the rhabdomere (Fig. 8 B). In contrast, shi^{ts2} *sec6(pr)* double mutants show cytoplasmic accumulation of Rh1 similar to *sec6(pr)* mutants (Fig. 8 C), suggesting that the cytoplasmic accumulation of Rh1 is not the result of increased endocytosis. In summary, these findings strongly argue for a direct Rab11/exocyst-dependent biosynthetic transport of Rh1 from the Golgi to the apical rhabdomere.

Discussion

Sec6 is critical for multiple secretory events during *Drosophila* development. PRCs provide a striking example. Secretory vesicles accumulate in PRCs with reduced Sec6 function and these cells fail to transport Rh1 and Chp to the rhabdomere. These defects in secretory activity lead to a corresponding failure in the growth of the membrane-rich rhabdomere. Sec6, similarly as previously reported for Sec5 (Murthy et al., 2003, Murthy and Schwarz, 2004), is also required for plasma membrane growth in female germline cells and cell survival. A recent independent analysis of *sec6* mutants confirms the function of Sec6 in cell viability and plasma membrane growth in the female germline, and indicates simi-

lar requirements for Sec6 and Sec5 in neuronal exocytosis (Murthy et al., 2005). These findings, together with the physical interactions between *Drosophila* Sec6 and Sec5 and the largely overlapping profiles of these proteins in a membrane cofractionation experiment suggest that both proteins are core components of the *Drosophila* exocyst.

The function of Sec6 in differentiating PRCs is specific to the targeting of secretory vesicles to the apical rhabdomere. The colocalization of Sec5, Sec6, and Sec8 at the rhabdomere suggests that all three exocyst components cooperate in this process. Although Sec6 is required for targeting Chp and Rh1 to the rhabdomere, it is not needed for DEcad and Crb localization to the ZA and stalk membrane, respectively, during the second half of PD. An alternative explanation for the normal localization of DEcad and Crb in *sec6(pr)* PRCs could be that both proteins are transported to the membrane in the first half of PD but not subsequently. However, this seems highly improbable, as it would imply that both proteins do not turn over any more. Also, the apical membrane of PRCs, including the Crb containing stalk membrane and the ZA, increases dramatically in the second half of PD, an increase that is most likely supported by protein exocytosis. Additional protein delivery is relevant in particular for Crb as the concentration of Crb determines the size of the stalk membrane (Pellikka et al., 2002). Failure to transport Rh1 and Chp in the absence of Sec6 is accompanied by an extensive accumulation of secretory vesicles in the cytoplasm of PRCs, similar to yeast cells that lack exocyst function (Novick et al., 1980). Rh1 transport is also reduced or abolished in PRCs that lack normal function of the small Rab GTPases, Rab1, Rab6, or Rab11. PRCs that lack Rab1 or Rab6 function do not accumulate secretory vesicles and these Rab proteins are believed to contribute to the ER to Golgi transport or inter-Golgi transport, respectively (Satoh et al., 1997; Shetty et al., 1998). Rab1 or Rab6 are therefore unlikely to directly interact with the exocyst in vesicle targeting to the rhabdomere.

In contrast to Rab1 and Rab6, Rab11-depleted PRCs accumulate secretory vesicles (Satoh et al., 2005) similar to *sec6(pr)* mutant PRCs, and Sec5 coimmunoprecipitates with Rab11::GFP from PRC and embryo lysates. These findings suggest that Rab11 takes the place of yeast Sec4p as the transport vesicle-associated small GTPase that recruits the exocyst (Guo et al., 1999). Although we detected Sec6 in Sec5 immunoprecipitates, we did not detect Sec6 in Rab11::GFP precipitates. We envision two explanations for this discrepancy. First, Rab11 may predominantly associate with a subcomplex of the exocyst that includes Sec5 but not Sec6. Second, in the yeast exocyst, Sec6p links to Sec4p through Sec15p, Sec10p, and Sec5p (Guo et al., 1999), suggesting that the Sec6 Rab11 interaction may involve several intermediates including Sec5 and therefore is more difficult to detect. Both explanations are consistent with the model that Sec5 connects Sec6 to Rab11, a relationship that is similar to the interactions of yeast exocyst components and Sec4p (Guo et al., 1999). Our results together with those of Satoh and colleagues (Satoh et al., 2005) suggest that the exocyst is a Rab11 effector complex in PRCs.

A more general role of the interaction of Rab11 and the exocyst in regulating exocytosis of metazoan cells is supported by a number of recent findings. First, Rab11 is associated with the RE (in epithelial cells often referred to as the apical RE or subapical compartment) and is involved in recycling of proteins in mammalian and *Drosophila* cells (Zerial and McBride, 2001; Dollar et al., 2002; Hoekstra et al., 2004). The RE has now been identified as a major intermediate for the biosynthetic, Rab11-dependent transport of basolateral proteins (Ang et al., 2004; Lock and Stow, 2005). For example, the majority of biosynthetic E-cadherin travels through the RE in a Rab11-dependent way in HeLa and MDCK cells (Lock and Stow, 2005). *Drosophila* Rab11 is also required for basolateral transport. Rab11 localizes to the RE in cellularizing embryos and facilitates the transport of proteins recycled from the apical membrane and biosynthetic proteins to the forming basolateral membrane (Riggs et al., 2003; Pelissier et al., 2003).

Second, the exocyst is required for basolateral protein transport including the targeting of E-cadherin to the basolateral membrane of MDCK cells (Grindstaff et al., 1998; Lipschutz et al., 2000). Whether the accumulation of *Drosophila* Sec6 at the ZA signifies a role for the exocyst in basolateral transport similar to MDCK cells (Grindstaff et al., 1998; Yeaman et al., 2004) remains to be established. Although we were unable to study the localization of basolateral markers in Sec6 mutant imaginal disc cells as they failed to grow, we observed that DEcad and DN-cadherin accumulate in the cytoplasm of *sec6* mutant epithelial follicle cells (unpublished data), which is consistent with a role of Sec6 in basolateral transport. Third, mammalian Sec15 was recently shown to directly bind to Rab11 in a GTP-dependent manner but did not interact with Rab4, Rab6 and Rab7, and Sec15 was found to colocalize with Rab11 in the RE of COS-7 cells (Zhang et al., 2004). Together, these data are consistent with the hypothesis that the exocyst is a Rab11 effector in many different cell types in mammals and flies that facilitates RE to plasma membrane transport of recycled and biosynthetic cargo. In *Drosophila* PRCs, the Rab11/exocyst transport of Rh1 appears to be predominantly biosynthetic as a block in endocytosis does not affect Rh1 delivery to the rhabdomere (Satoh et al., 2005; this work).

Considering the specific association of Sec6 with the ZA of early PRCs and a potentially broad role of Rab11/exocyst in basolateral transport it is tempting to speculate that during PRC development exocyst targeting specificity changes from basolateral to the apical rhabdomere. One possible explanation for this shift is that the exocyst associates with the actin cytoskeleton. As the vast majority of actin filaments in PRCs are found in the rhabdomere microvilli or the rhabdomere terminal web (Karagiosis and Ready, 2004) simple mass action via actin association could contribute to targeting specificity. The actin cytoskeleton is required in yeast to recruit the exocyst to secretory sites (Ayscough et al., 1997; Finger et al., 1998). Moreover, in the cells of pancreatic acini, exocyst proteins bind the actin cytoskeleton and this interaction is required for the association of the exocyst with Ca^{2+} signaling complexes that are targeted to the apical membrane (Shin et al., 2000). How shifts in exocyst targeting specificity are achieved is a major challenge for future research.

We have noted a number of differences in the distribution of Sec6, Sec5, and Sec8 in PRCs and during oogenesis that raise the possibility that exocyst proteins do not always act together. Also our cofractionation analysis shows a broader distribution of Sec6 than Sec5 and Sec8 indicating the association of Sec6 with additional membrane compartments. We cannot completely rule out the possibility that the observed differences in protein distribution are the result of differences in epitope availability of distinct exocyst protein pools. This issue has been raised by Yeaman et al. (2001), who report that mAbs directed against mammalian Sec6 and Sec8 recognize protein pools with different subcellular localizations. We believe that this is highly unlikely in our case as we use pAbs against Sec6 and Sec8. Moreover, each antibody we use recognizes cytoplasmic and plasma membrane-associated protein pools and either two or all three proteins are recognized when they colocalize as, for example, in the rhabdomere. Furthermore, inconsistencies in protein prevalence are also apparent by immunoblot and by cofractionation analysis. The ability of exocyst proteins to exist in subcomplexes was documented in yeast (Guo et al., 1999) and mammalian cells (Moskalenko et al., 2003). Also, biochemical studies of the interaction between Sec8, Sec6, and SAP102 in rat brain lysates suggested that Sec6 and Sec8 are not always present in the same complexes (Sans et al., 2003). The functional significance of these differences in the distribution of exocyst components needs to be addressed in future studies.

Materials and methods

Genetics and constructs

sec6 deletions were tested for complementation of the chromosomal deficiency *Df(2R)PC4* that completely removes *sec6*. *sec6* mutant clones in the germline were generated by crossing w^{1118}/Y; FRT^{42D} sec6/*SM6B* flies to w^{1118} hs-FLP; FRT^{42D} nls-GFP/*CyO* flies. Progeny were heat shocked for 2 h at 37°C either as third instar larvae or 0–6 h after eclosion. Flies were kept at 18°C for 24 h, and then for 48–96 h at 25°C before dissection. Whole-eye clones were made by crossing w^{1118}/Y; FRT^{42D} sec6/*SM6B* to *y* w^{1118}; FRT^{42D} GMR-hid l(2)Cl/*CyO*; *ey-Gal4*, *UAS-FLP* (Stowers and Schwarz, 1999). For *sec6(pr)* we added a third chromosomal *UAS-sec6* transgene to the aforementioned cross. shi^{ts2}/Y; *sec6(pr)* late pupae were incubated for 48–72 h at 29°C, and dissected at eclosion. arm^{XP33} clones were produced as described previously (Tanentzapf et al., 2000). *UAS-Rab11-GFP* flies are a gift of H. Chang (Purdue University, West Lafayette, IN). Rab11::GFP expression was induced by *Rh1-Gal4* (Kumar and Ready, 1995)) in adult heads and *da-Gal4* (Wodarz et al., 1995) in embryos. *UAS-sec6* was generated by first cloning a *sec6* cDNA with a full-length ORF by RT-PCR. Two cDNA fragments were amplified (primer pairs: forward 5′-GAATTCACTTCCACTGCTGACGAA-3′, reverse 5′-GCCAAAGATCTCCACCTGCTG-3′; and forward 5′-CAGCAGGTGGAGATCTTTGGC-3′, reverse 5′-GCTCTAGAATTTATTTGTTGATAAAGC-3′), combined and subcloned into pUASP (Rorth, 1998). Fly transformation followed standard methods.

Generation of Sec6 and Sec8 antibodies

A 500-bp BamHI–EcoRI fragment encoding aa 341–507, and a 1.9-kb EcoRI–XhoI piece encoding aa 152–738 of Sec6 were ligated into pRSETC (Invitrogen) and pGEX-6-P3 (Amersham Biosciences), respectively. A 750-bp BamHI–EcoRI fragment encoding aa 137–386 of Sec8 was subcloned into pRSETC. Proteins were expressed in BL21 cells, and purified using standard methods. pAbs against Sec8 and the Sec6 peptide (aa 341–507) were generated in guinea pigs and affinity purified. The larger Sec6 peptide (aa 152–738) was used to generate rabbit pAb (Covance).

Protein expression and immunoblotting

Dechorionated embryos, larvae, or adult retina were homogenized in SDS sample buffer (62.5 mM Tris-HCl, pH 6.8, 2.3% SDS, 10% glycerol, 5% β-mercaptoethanol, and 0.005% bromphenol blue). 50 μg of proteins were resolved by SDS-PAGE. Proteins were electro-transferred onto nitrocellulose membranes (Amersham Biosciences). Membranes were blocked in PBS containing 5% powdered milk and 0.05% Tween 20 for at least 1 h at 25°C. Membranes were incubated overnight at 4°C with primary antibodies in blocking solution and then with HRP-conjugated secondary antibody for 1 h at RT. After extensive washes in PBS containing 0.05% Tween 20, the blots were visualized using the ECL system (Amersham Biosciences). The following primary antibodies were used: mouse mAb anti–β-tubulin (E7, 1:5000; Chu and Klymkowsky, 1989), anti-GFP (JL-8, 1:2,000; CLONTECH Laboratories, Inc.), and anti-Sec5 (16A2, 1:250; Murthy et al., 2003); guinea pig pAbs anti-Sec6 (GP1, 1:2,000), and anti-Sec8 (GP3, 1:1,000); and rabbit pAb anti–α-spectrin (354, 1:2,000; a gift from D. Brandon, Harvard University, Cambridge, MA).

Co-immunoprecipitation experiments

Dechorionated embryos or adult heads were washed twice with ice-cold PBS and homogenized in chilled lysis buffer (50 mM NaCl, 50 mM NaF,1 mM EDTA, 40 mM Tris, pH 7.6, 1% Triton X-100,1 mM PMSF, 10 μg/ml leupeptin, 1 μg/ml pepstatin, 10 μg/ml aprotinin, 0.1 mM orthovanadate, and 40 mM β-glycerophosphate). Lysates were cleared of debris by centrifugation. mAb 16A2 (Sec5) and JL-8 (GFP) were added to 1 mg of lysate and incubated for 2 h at 4°C under agitation. 40 μg of protein G–Sepharose beads (Amersham Biosciences) were subsequently added for 1 h (16A2) or over night (JL-8) at 4°C under agitation. Immunocomplexes were harvested by centrifugation and washed four times with ice-cold lysis buffer. Proteins were solubilized with Laemmli buffer and separated by SDS-PAGE.

Membrane fractionation

Dechorionated embryos were rinsed in wash buffer (0.7% NaCl and 0.03% Triton X-100) and homogenized in 10 vol homogenization buffer (10 mM Tris, pH 7.5, 5 mM EDTA, 0.25 M sucrose, with protease inhibitors as in Sisson et al., 2000). KCl was added to a final concentration of 50 mM. After centrifugation at 3,000 *g* for 10 min at 4°C, the supernatant was layered on a sucrose cushion (15 mM Tris, pH 7.0, 50 mM KCl, 0.5 mM EDTA, 0.5 M sucrose) and centrifuged at 100,000 *g* for 1 h at 4°C. The supernatant was discarded and the loose pellet was resuspended and diluted fivefold in 10 mM Tris, pH 7.5, 5 mM EDTA, 50 mM KCl and membranes collected by centrifugation at 100,000 *g* for 1 h at 4°C. The pellet (load) was resuspended in homogenization buffer containing 50 mM KCl and mixed with OptiPrep medium (Accurate Chemical & Scientific Corp.) to prepare a 10–30% OptiPrep density gradient. After centrifugation (340,000 *g* for 3 h at 4°C), 0.25-ml fractions were collected from the bottom of the tube. 50 μg of the peak fraction and equal volumes of other gradient fractions were analyzed by immunoblotting.

Antibody staining and EM

The following primary antibodies were used: rat mAb anti-DEcad (DCAD2, 1:50; Oda et al., 1994), and anti–Dα-catenin (Dαcat; DCAT-1, 1:150; Oda et al., 1993); mouse mAb anti-Arm (N2-7A1, 1:100; Peifer et al., 1994), anti-Sec5 (16A2, 1:100; Murthy et al., 2003), anti-22C10 (22C10, 1:500; Fujita et al., 1982), anti-Chp (24B10, 1:50; Fujita et al., 1982), and anti-Rh1 (4C5, 1:50; Kumar and Ready, 1995), guinea pig pAb anti-Sec6 (GP1; serum, 1:1,000; affinity purified, 1:80), and anti-Sec8 (GP3; serum, 1:2,000; affinity purified, 1:500); rabbit pAb anti-Patj (1:250; Tanentzapf et al., 2000); and rat pAb anti-Crb (F1, 1:500; Pellikka et al., 2002). Secondary antibodies conjugated with Alexa Fluor-488 (Molecular Probes), Cy3, and Cy5 (Jackson Laboratories) were used at a dilution of 1:400. F-actin was stained with Alexa-546 and Alexa-488 phalloidin (Molecular Probes). Stainings of ovaries and retinas were done as reported previously (Niewiadomska et al., 1999; Tanentzapf et al., 2000; Pellikka et al., 2002). To stain membranes with Alexa Fluor-633–conjugated Con A (Molecular Probes) ovaries were incubated with 100 μg/ml in PBS for 30 min at RT. Tissues were mounted in antifade (PBS, pH 8.6, in 50% glycerol, and 25 mg/ml DABCO [Sigma-Aldrich]), or Vectashield (Vector Laboratories). Confocal images were taken on a LSM510 (Carl Zeiss, Inc.) at RT using Plan-Neofluar 40×/1.30 oil and Plan-Apochromat 100×/1.40 oil lenses. Images were processed in Adobe Photoshop or Adobe Illustrator. EM preparations were performed following standard protocols.

Online supplemental material

The online supplementary material shows the temporal expression profile of the *ey-Gal4* driver in the developing laval and pupal retina. Online supplemental material is available at http://www.jcb.org/cgi/content/full/jcb.200410081/DC1.

We are grateful to Henry Hong for technical assistance. We thank T. Schwarz, T. Uemura, H. Oda, M. Peifer, The Bloomington Drosophila Stock Center, and the Developmental Studies Hybridoma bank for reagents. We are grateful to Don Ready for discussion of unpublished results. We thank Dorothea Godt for critical reading of the manuscript.

This work was supported by a grant from the National Cancer Institute of Canada to U. Tepass, by a grant from the National Institute of Health (GM 067013) to J. Sisson, by a predoctoral fellowship from the Vision Science Research Program, University of Toronto to S. Beronja, and by a doctoral fellowship from the Fonds de la Recherche en Santé du Québec to P. Laprise.

Submitted: 15 October 2004
Accepted: 11 April 2005

References

Andrews, H.K., Y.Q. Zhang, N. Trotta, and K. Broadie. 2002. *Drosophila* sec10 is required for hormone secretion but not general exocytosis or neurotransmission. *Traffic.* 3:906–921.

Ang, A.L., T. Taguchi, S. Francis, H. Folsch, L.J. Murrells, M. Pypaert, G. Warren, and I. Mellman. 2004. Recycling endosomes can serve as intermediates during transport from the Golgi to the plasma membrane of MDCK cells. *J. Cell Biol.* 167:531–543.

Ayscough, K.R., J. Stryker, N. Pokala, M. Sanders, P. Crews, and D.G. Drubin. 1997. High rates of actin filament turnover in budding yeast and roles for actin in establishment and maintenance of cell polarity revealed using the actin inhibitor latrunculin-A. *J. Cell Biol.* 137:399–416.

Bucci, C., R.G. Parton, I.H. Mather, H. Stunnenberg, K. Simons, B. Hoflack, and M. Zerial. 1992. The small GTPase rab5 functions as a regulatory factor in the early endocytic pathway. *Cell.* 70:715–728.

Chu, D.T., and M.W. Klymkowsky. 1989. The appearance of acetylated alpha-tubulin during early development and cellular differentiation in *Xenopus*. *Dev. Biol.* 136:104–117.

Dollar, G., E. Struckhoff, J. Michaud, and R.S. Cohen. 2002. Rab11 polarization of the *Drosophila* oocyte: a novel link between membrane trafficking, microtubule organization, and oskar mRNA localization and translation. *Development.* 129:517–526.

Finger, F.P., and P. Novick. 1998. Spatial regulation of exocytosis: lessons from yeast. *J. Cell Biol.* 142:609–612.

Finger, F.P., T.E. Hughes, and P. Novick. 1998. Sec3p is a spatial landmark for polarized secretion in budding yeast. *Cell.* 92:559–571.

Fujita, S.C., S.L. Zipursky, S. Benzer, A. Ferrus, and S.L. Shotwell. 1982. Monoclonal antibodies against the *Drosophila* nervous system. *Proc. Natl. Acad. Sci. USA.* 79:7929–7933.

Grigliatti, T.A., L. Hall, R. Rosenbluth, and D.T. Suzuki. 1973. Temperature-sensitive mutations in *Drosophila melanogaster*. XIV. A selection of immobile adults. *Mol. Gen. Genet.* 120:107–114.

Grindstaff, K.K., C. Yeaman, N. Anandasabapathy, S.C. Hsu, E. Rodriguez-Boulan, R.H. Scheller, and W.J. Nelson. 1998. Sec6/8 complex is recruited to cell-cell contacts and specifies transport vesicle delivery to the basal-lateral membrane in epithelial cells. *Cell.* 93:731–740.

Guo, W., D. Roth, C. Walch-Solimena, and P. Novick. 1999. The exocyst is an effector for Sec4p, targeting secretory vesicles to sites of exocytosis. *EMBO J.* 18:1071–1080.

Hazuka, C.D., D.L. Foletti, S.C. Hsu, Y. Kee, F.W. Hopf, and R.H. Scheller. 1999. The sec6/8 complex is located at neurite outgrowth and axonal synapse-assembly domains. *J. Neurosci.* 19:1324–1334.

Hoekstra, D., D. Tyteca, and S.C. van IJzendoorn. 2004. The subapical compartment: a traffic center in membrane polarity development. *J. Cell Sci.* 117:2183–2192.

Hsu, S.C., D. TerBush, M. Abraham, and W. Guo. 2004. The exocyst complex in polarized exocytosis. *Int. Rev. Cytol.* 233:243–265.

Inoue, M., L. Chang, J. Hwang, S.H. Chiang, and A.R. Saltiel. 2003. The exocyst complex is required for targeting of Glut4 to the plasma membrane by insulin. *Nature.* 422:629–633.

Karagiosis, S.A., and D.F. Ready. 2004. Moesin contributes an essential structural role in *Drosophila* photoreceptor morphogenesis. *Development.* 131:725–732.

Kumar, J.P., and D.F. Ready. 1995. Rhodopsin plays an essential structural role in *Drosophila* photoreceptor development. *Development.* 121:4359–4370.

Lipschutz, J.H., and K.E. Mostov. 2002. Exocytosis: the many masters of the exocyst. *Curr. Biol.* 12:R212–R214.

Lipschutz, J.H., W. Guo, L.E. O'Brien, Y.H. Nguyen, P. Novick, and K.E. Mostov. 2000. Exocyst is involved in cystogenesis and tubulogenesis and acts by modulating synthesis and delivery of basolateral plasma membrane and secretory proteins. *Mol. Biol. Cell.* 11:4259–4275.

Littleton, J.T. 2000. A genomic analysis of membrane trafficking and neurotransmitter release in *Drosophila. J. Cell Biol.* 150:F77–F82.

Lock, J.G., and J.L. Stow. 2005. Rab11 in recycling endosomes regulates the sorting and basolateral transport of E-cadherin. *Mol. Biol. Cell.* 16:1744–1755.

Longley, R.L., Jr., and D.F. Ready. 1995. Integrins and the development of three-dimensional structure in the *Drosophila* compound eye. *Dev. Biol.* 171:415–433.

Moskalenko, S., C. Tong, C. Rosse, G. Mirey, E. Formstecher, L. Daviet, J. Camonis, and M.A. White. 2003. Ral GTPases regulate exocyst assembly through dual subunit interactions. *J. Biol. Chem.* 278:51743–51748.

Mostov, K., T. Su, and M. ter Beest. 2003. Polarized epithelial membrane traffic: conservation and plasticity. *Nat. Cell Biol.* 5:287–293.

Murthy, M., and T.L. Schwarz. 2004. The exocyst component Sec5 is required for membrane traffic and polarity in the *Drosophila* ovary. *Development.* 131:377–388.

Murthy, M., D. Garza, R.H. Scheller, and T.L. Schwarz. 2003. Mutations in the exocyst component Sec5 disrupt neuronal membrane traffic, but neurotransmitter release persists. *Neuron.* 37:433–447.

Murthy, M., R. Ranjan, N. Denef, M.E. Higashi, T. Schüpbach, and T.L. Schwarz. 2005. Sec6 mutations and the *Drosophila* exocyst complex. *J. Cell Sci.* 118:1139–1150.

Niewiadomska, P., D. Godt, and U. Tepass. 1999. DE-Cadherin is required for intercellular motility during *Drosophila* oogenesis. *J. Cell Biol.* 144:533–547.

Novick, P., C. Field, and R. Schekman. 1980. Identification of 23 complementation groups required for post-translational events in the yeast secretory pathway. *Cell.* 21:205–215.

Oda, H., T. Uemura, K. Shiomi, A. Nagafuchi, S. Tsukita, and M. Takeichi. 1993. Identification of a *Drosophila* homologue of alpha-catenin and its association with the armadillo protein. *J. Cell Biol.* 121:1133–1140.

Oda, H., T. Uemura, Y. Harada, Y. Iwai, and M. Takeichi. 1994. A *Drosophila* homolog of cadherin associated with armadillo and essential for embryonic cell-cell adhesion. *Dev. Biol.* 165:716–726.

Pavel, J., C. Harter, and F.T. Wieland. 1998. Reversible dissociation of coatomer: functional characterization of a beta/delta-coat protein subcomplex. *Proc. Natl. Acad. Sci. USA.* 95:2140–2145.

Peifer, M., D. Sweeton, M. Casey, and E. Wieschaus. 1994. wingless signal and Zeste-white 3 kinase trigger opposing changes in the intracellular distribution of Armadillo. *Development.* 120:369–380.

Pelissier, A., J.P. Chauvin, and T. Lecuit. 2003. Trafficking through Rab11 endosomes is required for cellularization during *Drosophila* embryogenesis. *Curr. Biol.* 13:1848–1857.

Pellikka, M., G. Tanentzapf, M. Pinto, C. Smith, C.J. McGlade, D.F. Ready, and U. Tepass. 2002. Crumbs, the *Drosophila* homologue of human CRB1/RP12, is essential for photoreceptor morphogenesis. *Nature.* 416:143–149.

Prigent, M., T. Dubois, G. Raposo, V. Derrien, D. Tenza, C. Rosse, J. Camonis, and P. Chavrier. 2003. ARF6 controls post-endocytic recycling through its downstream exocyst complex effector. *J. Cell Biol.* 163:1111–1121.

Quiring, R., U. Walldorf, U. Kloter, and W.J. Gehring. 1994. Homology of the eyeless gene of *Drosophila* to the Small eye gene in mice and Aniridia in humans. *Science.* 265:785–789.

Riggs, B., W. Rothwell, S. Mische, G.R. Hickson, J. Matheson, T.S. Hays, G.W. Gould, and W. Sullivan. 2003. Actin cytoskeleton remodeling during early *Drosophila* furrow formation requires recycling endosomal components nuclear-fallout and Rab11. *J. Cell Biol.* 163:143–154.

Rodriguez-Boulan, E., A. Musch, and A. Le Bivic. 2004. Epithelial trafficking: new routes to familiar places. *Curr. Opin. Cell Biol.* 16:436–442.

Rorth, P. 1998. Gal4 in the *Drosophila* female germline. *Mech. Dev.* 78:113–118.

Rorth, P., K. Szabo, A. Bailey, T. Laverty, J. Rehm, G.M. Rubin, K. Weigmann, M. Milan, V. Benes, W. Ansorge, and S.M. Cohen. 1998. Systematic gain-of-function genetics in *Drosophila. Development.* 125:1049–1057.

Sang, T.K., and D.F. Ready. 2002. Eyes closed, a *Drosophila* p47 homolog, is essential for photoreceptor morphogenesis. *Development.* 129:143–154.

Sans, N., K. Prybylowski, R.S. Petralia, K. Chang, Y.X. Wang, C. Racca, S. Vicini, and R.J. Wenthold. 2003. NMDA receptor trafficking through an interaction between PDZ proteins and the exocyst complex. *Nat. Cell Biol.* 5:520–530.

Satoh, A., F. Tokunaga, S. Kawamura, and K. Ozaki. 1997. In situ inhibition of vesicle transport and protein processing in the dominant negative Rab1 mutant of *Drosophila. J. Cell Sci.* 110:2943–2953.

Satoh, A.L., J.E. O'Tousa, K. Ozaki, and D.F. Ready. 2005. Rab11 mediates post-Golgi trafficking of rhodopsin to the photosensitive apical membrane of *Drosophila* photoreceptors. *Development*. 132:1487–1497.

Schuck, S., and K. Simons. 2004. Polarized sorting in epithelial cells: raft clustering and the biogenesis of the apical membrane. *J. Cell Sci.* 117:5955–5964.

Shetty, K.M., P. Kurada, and J.E. O'Tousa. 1998. Rab6 regulation of rhodopsin

transport in *Drosophila. J. Biol. Chem.* 273:20425–20430.

Shimizu, H., S. Kawamura, and K. Ozaki. 2003. An essential role of Rab5 in uniformity of synaptic vesicle size. *J. Cell Sci.* 116:3583–3590.

Shin, D.M., X.S. Zhao, W. Zeng, M. Mozhayeva, and S. Muallem. 2000. The mammalian Sec6/8 complex interacts with Ca^{2+} signaling complexes and regulates their activity. *J. Cell Biol.* 150:1101–1112.

Sisson, J.C., C. Field, R. Ventura, A. Royou, and W. Sullivan. 2000. Lava lamp, a novel peripheral Golgi protein, is required for *Drosophila melanogaster* cellularization. *J. Cell Biol.* 151:905–918.

Stanley, H., J. Botas, and V. Malhotra. 1997. The mechanism of Golgi segregation during mitosis is cell type-specific. *Proc. Natl. Acad. Sci. USA.* 94:14467–14470.

Stowers, R.S., and T.L. Schwarz. 1999. A genetic method for generating *Drosophila* eyes composed exclusively of mitotic clones of a single genotype. *Genetics.* 152:1631–1639.

Tanentzapf, G., C. Smith, J. McGlade, and U. Tepass. 2000. Apical, lateral, and basal polarization cues contribute to the development of the follicular epithelium during *Drosophila* oogenesis. *J. Cell Biol.* 151:891–904.

van der Bliek, A.M., and E.M. Meyerowitz. 1991. Dynamin-like protein encoded by the *Drosophila* shibire gene associated with vesicular traffic. *Nature.* 351:411–414.

Van Vactor, D., Jr., D.E. Krantz, R. Reinke, and S.L. Zipursky. 1988. Analysis of mutants in chaoptin, a photoreceptor cell-specific glycoprotein in *Drosophila*, reveals its role in cellular morphogenesis. *Cell.* 52:281–290.

Vega, I.E., and S.C. Hsu. 2001. The exocyst complex associates with microtubules to mediate vesicle targeting and neurite outgrowth. *J. Neurosci.* 21:3839–3848.

Wodarz, A., U. Hinz, M. Engelbert, and E. Knust. 1995. Expression of crumbs confers apical character on plasma membrane domains of ectodermal epithelia of *Drosophila. Cell.* 82:67–76.

Yeaman, C., K.K. Grindstaff, J.R. Wright, and W.J. Nelson. 2001. Sec6/8 complexes on trans-Golgi network and plasma membrane regulate late stages of exocytosis in mammalian cells. *J. Cell Biol.* 155:593–604.

Yeaman, C., K.K. Grindstaff, and W.J. Nelson. 2004. Mechanism of recruiting Sec6/8 (exocyst) complex to the apical junctional complex during polarization of epithelial cells. *J. Cell Sci.* 117:559–570.

Zerial, M., and H. McBride. 2001. Rab proteins as membrane organizers. *Nat. Rev. Mol. Cell Biol.* 2:107–117.

Zhang, X.M., S. Ellis, A. Sriratana, C.A. Mitchell, and T. Rowe. 2004. Sec15 is an effector for the Rab11 GTPase in mammalian cells. *J. Biol. Chem.* 279:43027–43034.